Available online at www.sciencedirect.com
ScienceDirect
Bioorganic & Medicinal Chemistry Letters 17 (2007) 2351–2354
Bioorganic & Medicinal Chemistry Letters

Fluorinated NSC as a Cdc25 inhibitor

Hwangseo Park,[a] Brian I. Carr,[b] Minghua Li[c] and Seung Wook Ham[c,*]

[a]*Department of Bioscience and Biotechnology, Sejong University, 98 Kunja-Dong, Kwangjin-Ku, Seoul 143-747, Republic of Korea*
[b]*Liver Cancer Center, Starzl Transplantation Institute, University of Pittsburgh Medical Center, Pittsburgh, PA 15213, USA*
[c]*Department of Chemistry, Chung-Ang University, Seoul 156-756, Republic of Korea*

Received 11 September 2006; revised 17 November 2006; accepted 12 December 2006
Available online 21 December 2006

Abstract—We report on the fluorinated form of NSC 95397 as a Cdc25B inhibitor, which is predicted to be only an arylator of cysteine-containing proteins, without generating reactive oxygen species.

Cdc25 phosphatases are important in cell cycle control and activate cyclin-dependent kinases (Cdk). Among three Cdc25 homologues in humans, Cdc25A and Cdc25B have oncogenic properties and are overexpressed in various human tumors,[1] which makes them attractive drug targets for anticancer therapies. Among the numerous published molecules, only few were found to possess potency against Cdc25s.[2] To date, the most potent Cdc25 inhibitor was quinone-containing NSC 95397 from the National Cancer Institute library.[3] More recently, we synthesized two hydroxyl derivatives of NSC 95397, monohydroxyl-NSC 95397 (M-NSC) and dihydroxyl-NSC 95397 (D-NSC), which both have enhanced activity for inhibiting Cdc25s.[4] The new analogues, D-NSC in particular, potently inhibited the growth of human hepatoma and breast cancer cells in vitro.

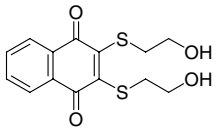

NSC 95397 (1)

Although most quinones have been reported to inhibit Cdc25 by sulfhydryl arylation at the quinone nucleus, the redox properties of the quinones can also generate toxic oxygen species,[5] which may cause toxicity to normal tissues and thus reduce their therapeutic attractiveness.[6] Regarding oxidative stress of quinones, the relative one-electron reduction potentials of quinones control the position of the equilibrium defining 'futile cycling':[7]

$$Q^{\cdot-} + O_2 \rightleftharpoons Q + O_2^{\cdot-}$$

Since the equilibrium constant of the above reaction is approximately equal to $10^{\Delta E/0.06}$ where ΔE is the difference in one-electron reduction potentials of oxygen (−0.155 V) and quinone,[8] the superoxide formation will be increasingly favored as the reduction potential of quinone decreases.

In this study, we have extended the investigation to fluorinated NSC 95397 (F-NSC) whose reduction potential is expected to be higher than that for NSC 95397. This is due to the inductive effects of the electronegative fluorine atoms that prevent superoxide generation. Since direct treatment of commercially available hexafluoronaphthoquinone with β-mercaptoethanol resulted in the intramolecular cyclized product, O-protected β-mercaptoethanol was added to methanolic solution of hexafluoronaphthoquinone. The reaction mixture was stirred at room temperature for 20 min, treated with toluenyl sulfonyl acid, and stirred for another 30 min. After concentration under reduced pressure, the resulting crude product was purified by column chromatography on SiO_2 (hexane/ethyl acetate, 2:1) to give the desired product **3**. Chemical structure was confirmed by infrared spectroscopy, ^1H NMR, and high-resolution mass spectrum analysis.

Keywords: Cdc25 phosphatase; Inhibitor; Antitumor; Quinones; Modeling.
* Corresponding author. Tel.: +82 2 820 5203; fax: +82 2 825 4736; e-mail: swham@cau.ac.kr

0960-894X/$ - see front matter © 2007 Elsevier Ltd. All rights reserved.
doi:10.1016/j.bmcl.2006.12.046

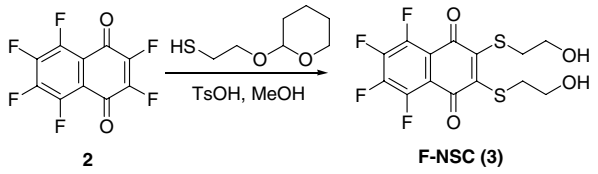

This compound was then tested for its inhibitory activity against Cdc25B. NSC 95397 is known to inhibit the dephosphorylation of *O*-methyl fluorescein phosphate (OMFP) with an IC_{50} of 0.1 μM.[3] Keeping it in mind that the kinetics of enzyme inhibitions depend on the choice of substrate as well as the domain of the enzyme, we measured the inhibitory activity of the newly synthesized compound for the GST-fusion Cdc25B in comparison with NSC 95397 by using the substrate *p*-nitrophenylphosphate in common. As shown in Figure 1, F-NSC was more potent than NSC 95397 in its ability to inhibit Cdc25B. Figure 2 depicts the time course of inhibition in the presence of increasing concentration of F-NSC.

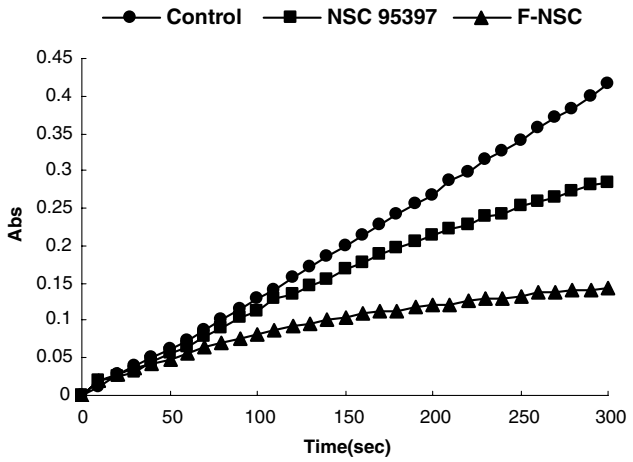

Figure 1. Purified GST-Cdc25B phosphatase was incubated with the chromogenic substrate, 40 μM *p*-nitrophenylphosphate, in 20 mM Tris (pH 8.0), 1 mM EDTA, and 0.2 mM DTT. To determine the efficiency of enzyme inhibition by 10 μM NSC 95397 and F-NSC, we continuously monitored at 410 nm and 37 °C by UV/vis spectrophotometer equipped with a thermostatic cell holder.

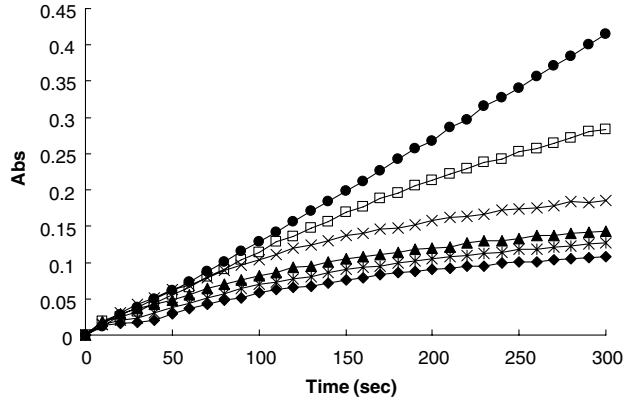

Figure 2. Time course of the reaction of GST-Cdc25B phosphatase in the absence of or presence of F-NSC (1, 5, 10, 20, and 40 μM).

Like NSC 95397 as well as naphthoquinone-containing Cdc25 inactivators such as menadione and Compd **5**, the activity of inactivated enzyme with F-NFC did not return after dialysis, suggesting an irreversible inactivation by arylation.

Several reductases can reduce the quinones by one-electron or two-electron transfer to form the semiquinone and hydroquinone, respectively. Both the semiquinone and the hydroquinone can then reduce oxygen, resulting in the formation of superoxide anion. However, it has been reported that NSC 95397-generated cytotoxicity was unaffected by NAD(P)H:quinone oxidoreductase-1 (NQO1),[9] two-electron reduction enzyme. Therefore, only single electron transfer to NSCs by enzymes such as NADH-cytochrome P450 oxidoreductase, NADH-cytochrome b_5 oxidoreductase, and NADH-ubiquinone oxidoreductase is possible to generate the reactive oxygen species. To estimate the stability of the semiquinone form of F-NSC, the reduction potential of F-NSC was determined by cyclic voltammetry. $E_{1/2}$ of F-NSC solution amounted to 236 mV in an acetonitrile containing tetra-*n*-butylammonium perchlorate as the supporting electrolyte, which is referred to as an Ag/Ag^+ redox couple. This result indicates the relative stability of semiquinone as compared to the superoxide anion.

To gain structural insight into the inhibitory mechanisms of NSC 95397 and its derivatives for Cdc25B, docking simulations were carried out with AutoDock program[10] in the active site of Cdc25B. The probed compounds included F-NSC as well as NSC 95397 and the hydroxy derivative of NSC 95397 (D-NSC). The potential grids of dimension $61 \times 61 \times 61$ points with the spacing of 0.375 Å were used in the docking simulations, which yield a receptor model that includes the atoms within 22.9 Å of the grid center located in the active site around Cys473. To calculate the intermolecular electrostatic interactions, Gasteiger–Marsili charges were assigned to all protein and ligand atoms. Initial step sizes for translational and torsional motions of a ligand were set equal to 2.0 Å and 50.0°, respectively.

With respect to the determination of protonation states of the ionizable residues, we used the atomic distance data in the X-ray structure of CDC25B. For example, the sidechains of Asp and Glu residues were assumed to be neutral if their carboxylate oxygens of OD or OE atoms were located within 3.5 Å from a hydrogen-bond accepting group including the backbone aminocarbonyl oxygen. Similarly, the sidechains of lysine and histidine were assumed to be protonated unless their respective nitrogen atom was in proximity of a hydrogen-bond donating group. In this way Cys473 and Glu474 were assumed to be ionized, while ND1 and NE2 atoms of His472 appeared to be protonated and deprotonated, respectively.

Prior to the actual docking simulations, the original X-ray crystal structure of Cdc25B was equilibrated in

aqueous solution through 0.5 ns molecular dynamics simulation with AMBER program.[11] The equilibration procedure started with the addition of one sodium ion as the counterion to neutralize the total charge of the all-atom model of Cdc25B. The system was then immersed in a rectangular solvent box containing 6994 TIP3P water molecules. After 1000 cycles of energy minimization to remove bad van der Waals contacts, we equilibrated the system beginning with 20 ps equilibration dynamics of the solvent molecules at 300 K. The next step involved equilibration of the solute with a fixed configuration of the solvent molecules for 10 ps at 10, 50, 100, 150, 200, 250, and 300 K. Then, the equilibration dynamics of the entire system was performed at 300 K for 500 ps using the periodic boundary condition. The SHAKE algorithm[12] was applied to fix all bond lengths involving hydrogen atom. We used a time step of 1.5 fs and a nonbond-interaction cutoff radius of 12 Å.

Table 1 lists the calculated binding free energies of the three Cdc25B inhibitors under investigation. Keeping it in mind that the binding free energy of a protein–ligand complex in solution (ΔG^{sol}_{bind}) can be approximated as the difference between that in the gas phase (ΔG^{gas}_{bind}) and the solvation free energy of the ligand (ΔG^{sol}),[13] we computed the two energy components separately to estimate their relative contributions to ΔG^{sol}_{bind}. We note that ΔG^{gas}_{bind} becomes more favorable with the introduction of the two hydroxy groups in the phenyl ring. Simultaneously, however, the solvation free energy becomes more negative, leading to an insignificant change in ΔG^{sol}_{bind} between NSC 95397 and D-NSC. These results indicate that the increased stabilization in solution due to structural changes should be overcome by an even stronger enzyme–inhibitor interaction in order to enhance the inhibitory activity. F-NSC is predicted to be a more potent inhibitor than NSC 95397 due to a strengthening of the enzyme–inhibitor interaction and a little destabilization in solution, which is consistent with experimental data shown in Figures 1 and 2.

Shown in Figure 3 are the calculated binding modes of the three inhibitors in the active site of Cdc25B. It is noted that NSC 95397 fits the active site pocket with one of its carbonyl groups pointing toward Cys473. The two terminal hydroxy groups form hydrogen bonds with the sidechain of Glu474 and the backbone –NH group of Ser477. The inhibitor is further stabilized in the active site by the hydrophobic interaction of the phenyl ring with the sidechain of Tyr428. The binding mode found in this study differs from that of the earlier docking results reported by Lazo et al.[3] and that found in the recent docking study by Lavecchia et al.[14] in which the

Table 1. Calculated binding free energy in the gas phase, solvation free energy, and binding free energy in solution for the three Cdc25B inhibitors[a]

Inhibitors	ΔG^{gas}_{bind}	ΔG^{sol}	ΔG^{sol}_{bind}
NSC 95397	−17.74	−3.51	−14.23
D-NSC	−19.43	−5.14	−14.29
Fluorinated NSC	−18.17	−3.30	−14.87

[a] All energy values are given in kcal/mol.

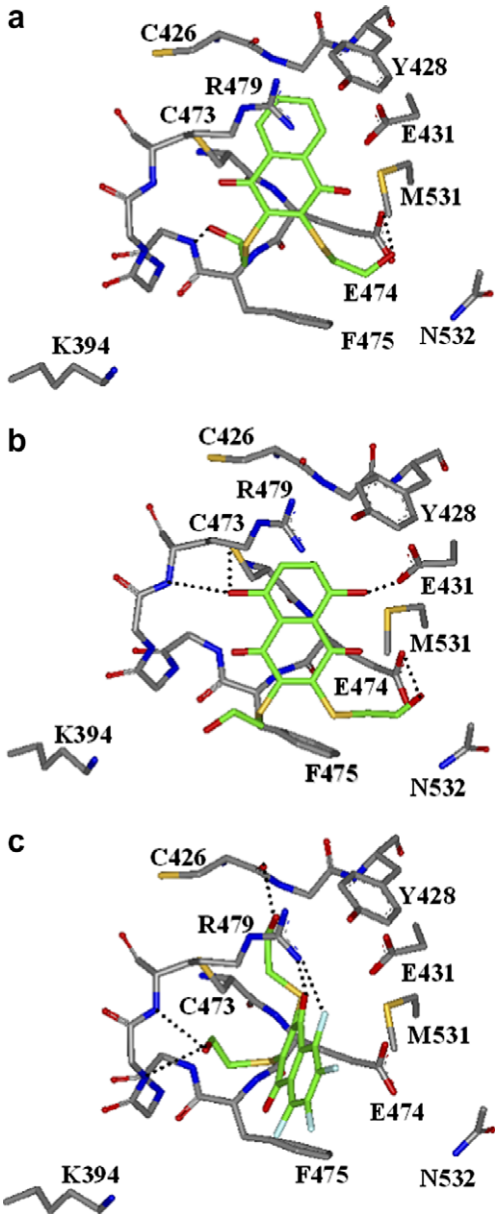

Figure 3. Comparative view of the binding modes of (a) NSC95397, (b) D-NSC, and (c) F-NSC. Yellow dotted lines indicate a hydrogen bond established from the inhibitor and the active site residues of Cdc25B.

naphthoquinone moiety of the inhibitors could not be accommodated in the active site. This stems from the use of the original X-ray crystal structure without an appropriate refinement to remove bad van der Waals contacts. It is thus likely that the binding mode reported in the current study could be more relevant to the inhibitory activity of NSC 95397 against Cdc25B. As can be seen in Figure 3b, the derivatization of hydroxy groups at the phenyl ring of NSC 95397 leads to the formation of additional hydrogen bonds with the sidechains of Cys473 and Glu431, as well as the backbone amide groups that reside at the active site. These newly formed hydrogen bonds may have an effect of stabilizing the enzyme–inhibitor complexes. However, the increase in inhibitory activities of the two derivatized compounds is expected to be limited by the simultaneous increase

in desolvation cost for binding to the enzymatic active site (Table 1). F-NSC exhibits a quite different binding mode from the others in that the two hydroxylated alkyl chains are bound in the active site with the ring group being exposed to bulk solvent. One of the two terminal hydroxy groups forms bifurcated hydrogen bonds with the backbone amide groups of Glu478 and Arg479, while the other acts as hydrogen-bond donor to the backbone aminocarbonyl group of Cys426. A bifurcated hydrogen bond is also established between Arg479 and one of the carbonyl oxygens and fluorine atoms of F-NSC. Judging from the higher potency of F-NSC compared with NSC 95397, the formation of multiple hydrogen bonds seems to successfully compensate for the loss of favorable hydrophobic interactions involving the aromatic groups of the protein and the inhibitor. This may in turn explain the difference in the binding mode of F-NSC.

Acknowledgment

This work was supported by the Seoul R&BD Program.

References and notes

1. For review, see: (a) Boutros, R.; Dozier, C.; Ducommun, B. *Curr. Opin. Cell Biol.* **2006**, *18*, 185; (b) Kristjansdottir, K.; Rudolph, J. *Chem. Biol.* **2004**, *11*, 1043.
2. For review, see: (a) Eckstein, J. W. *Invest. New Drugs* **2000**, *18*, 149; (b) Pesttell, K. E.; Ducruet, A. P.; Wipf, P.; Lazo, J. S. *Oncogene* **2002**, *19*, 6607; (c) Lyon, M. A.; Ducruet, A. P.; Wipf, P.; Lazo, J. S. *Nat. Rev. Drug Discov.* **2002**, *1*, 961.
3. Lazo, J. S.; Nemoto, K.; Pestell, K. E.; Cooley, K.; Southwick, E. C.; Mitchell, D. A.; Furey, W.; Gussio, R.; Zaharevitz, D. W.; Joo, B.; Wipf, P. *Mol. Pharmacol.* **2002**, *61*, 720.
4. Peyegene, V. P.; Kar, S.; Ham, S. W.; Wanf, M.; Wang, Z.; Carr, B. I. *Mol. Cancer Ther.* **2005**, *4*, 595.
5. Wardman, P. *Curr. Med. Chem.* **2001**, *8*, 739.
6. Morrison, H.; Jernström, B.; Nordenskjold, M.; Thor, H.; Orrenius, S. *Biochem. Pharmacol.* **1984**, *33*, 1763.
7. Hochstein, P. *Fundam. Appl. Toxicol.* **1983**, *3*, 215.
8. Wardman, P. *J. Phys. Chem. Ref. Data* **1989**, *18*, 1637.
9. Han, Y.; Shen, H.; Carr, B. I.; Wipf, P.; Lazo, J. S.; Pan, S. S. *J. Pharmacol. Exp. Ther.* **2004**, *309*, 64.
10. Morris, G. M.; Goodsell, D. S.; Halliday, R. S.; Huey, R.; Hart, W. E.; Belew, R. K.; Olson, A. J. *J. Comput. Chem.* **1998**, *19*, 1639.
11. Case, D. A.; Cheatham, T. E., III; Darden, T.; Gohlke, H.; Luo, R.; Merz, K. M., Jr.; Onufriev, A.; Simmerling, C.; Wang, B.; Woods, R. J. *J. Comput. Chem.* **2005**, *26*, 1668.
12. Ryckaert, J. P.; Ciccotti, G.; Berendsen, H. C. *J. Comput. Phys.* **1977**, *23*, 327–341.
13. Shoichet, B. K.; Leach, A. R.; Kuntz, I. D. *Proteins* **1999**, *34*, 4.
14. Lavecchia, A.; Cosconati, S.; Limongelli, V.; Novellino, E. *Chem. Med. Chem.* **2006**, *1*, 540–550.